# RAMAN SPECTRA, PHYSICAL PARAMETERS AND MICROHARDNESS OF GLASSES WITH COMPOSITION: $TeO_2$-$V_2O_5$-$Li_2O$

I. M. ASHRAF[a,b], M. FAROUK[c], F. AHMAD[d], M. M. EL OKR[c], M. M. ABDE - AZIZ[c], E. YOUSEF[a,e*]

[a]*PhysicsDep., Faculty of Science, King Khalid University, P. O. Box 9004, Abha, SaudiArabia*

[b]*PhysicsDep., Faculty of Sciences,AswanUniversity, Aswan, Egypt*

[c]*Physics Department, Faculty of Science, Al- Azahr University, Nasr city, Cairo, Egypt*

[d]*Physics Department, Faculty of Science, Al- Azahr University (Girls Branch), Nasr City, Cairo, Egypt*

[e]*Physics Department, Faculty of Science, Al- Azahr University,Assuit Branch, Egypt*

Ternary tellurovanadate glass samples with composition of (90-x) $TeO_2$-x$V_2O_5$-10$Li_2O$ (x= 20, 30, 40, 50, 60, and 70 mol%) were prepared using melt-quenching technique. The structure analysis was carried out using X-ray diffraction XRD and Raman spectroscopy. The density, molar volume, oxygen molar volume, and oxygen packing density were calculated. Vickers method was used to measure the microhardness. XRD patterns and FT-Raman confirm that there is no sharp peak and all samples have amorphous nature. The density and the oxygen molar volume ($V_o$) of the glassy testers decreases from 4.58 to 3.41 g.cm$^{-3}$ and from 12.81 to 11.25 cm$^3$, respectively, with increasing the mole% of $V_2O_5$. In addition, the rigidity of the samples was reduced according to the microhardness measurements.

(Received April 12, 2019; Accepted September 13, 2019)

*Keywords:* Tellurovanadate, XRD,Physical parameters,Semiconducting;glasses, Activation energy

## 1. Introduction

Tellurite based glasses are of technological interest due to its special properties such aslow melting point, high linear and non-linear refractive indices, high chemical durability, low crystallization, large infrared transparency, good thermal stability, corrosion resistance, and suitability as a matrix for active element doping for various applications[1-3]. Tellurium oxide $TeO_2$ is a conditional glass former, and does not form glass smoothly when it is melted as pure [4,5]. Therefore, it is necessary to add other components to reach the glass state. However, the addition of a glass forming agents or modifiers such as alkali oxides, heavy metal oxidesand transitional metal oxides (TMO) or other glass formers into the $TeO_2$ enhance the ability to form tellurite glass [6,7].

The structure of tellurite based glasses consists of $TeO_4$ trigonal bipyramids (tbp) (two oxygen ions are existing in the axial vertices, however the other two oxygen ions and the tellurium lone electron pair occupythe Te $sp^3d$ equatorial site), $TeO_{3+1}$ polyhedra (the subscript (3 + 1) indicates that the oxygen atom is bonded to tellurium atom but far from it compared to the other three oxygen atoms), and $TeO_3$ trigonal pyramids (tp) ($TeO_3$ trigonal pyramids (tp) structure consists of two bridging oxygen sites (alone pair of electrons occupies the apex of the Te $sp^3$ orbital) and one nonbridging oxygen atom) as the main structure units [8,9].The concentration of

*Corresponding authors: omn_yousef2000@yahoo.com

these structural units in the glass network depends on the type and the concentration of the glass modifier. When network modifier oxides are addedto $TeO_2$, Te – O – Te or O – Te – O network bridges are broken accompanied by the formation of non-bridging oxygen sites.The addition of transition metals oxide has a great interest because of their potential application. Such as vanadium pentoxide $V_2O_5$. Tellurovanadate ($TeO_2$ – $V_2O_5$) glasses have special properties due to their semiconducting behavior, due to hopping of polarons between $V^{4+}$ and $V^{5+}$ ions [10]. So, conduction can occur by ions transfer from lower valance state to a higher valance state. The structural properties of tellurite glasses with semiconducting transition metals are studied early with previous researchers [11,12], due to there several applications in electronics and industries. Addition of $V_2O_5$ is another glass former to tellurite glass, which depends on the concentration of $V_2O_5$. When $V_2O_5$< 20 mol%, the glass is tellurite network. While, when $V_2O_5$> 20 mol% the network transforms to vanadate glass [13]. Several studies observed that, as the concentration of $V_2O_5$ increases the nonbridging oxygens increases [14,15]. The structural and physical properties of the binary $TeO_2$ – $V_2O_5$ glasses have been investigated [16,17].

There are several reports about the physical properties of ternary Telluro – vanadate glassy systems including the third component ofNiO [18], $Ag_2O$ [19],CuO[20], and $K_2O$[21]. Lithium oxide $Li_2O$ is an interesting material due to its useful electronic properties [22]. Krins et al. [23], and Frechero et al. [24] studied the structure of $xLi_2O.(1\text{-}x)$ $(0.3V_2O_5 – 0.7TeO_2)$ and $xLi_2O.(1\text{-}x)$ $V_2O_5.2TeO_2$glasses, showed that the addition of $Li_2O$ causes the splitting of V – O – V and O – Te – O bonds, and also increase of the non – bridging oxygens (NBOs) concentration.

Based on the previous studies, the structure analysis of $[(90 – x)\ TeO_2 – xV_2O_5 – 10Li_2O]$ glasswith increasing $V_2O_5$content is investigated, using X-ray diffraction (XRD) and Raman spectroscopy.The structural parameters such as density, molar volume, oxygen molar volume, oxygen packing density, and microhardness were calculated.

## 2. Experimental procedures

### 2.1. Glass preparation

The ternary tellurovanadate glass samples with starting composition of $[(90 – x)\ TeO_2 – xV_2O_5 – 10Li_2O]$ here (x = 20, 30, 40, 50, 60 and 70 mol%) were prepared by mixing specified weights of vanadium pentoxide ($V_2O_5$, 99.6% purity, Sigma Aldrich), tellurium dioxide ($TeO_2$, 99.99% purity, Alfa Aesar), and lithium oxide ($Li_2O$, 97% purity, Sigma Aldrich).All samples were prepared using the melt-quenching technique. An appropriate amount of $V_2O_5$, $TeO_2$ and $Li_2O$ powder was mixed in a platinum crucible. The 20g batches of the mixture were preheated at a temperature of 980 $^oC$ in a furnace for 40 min to improve homogeneity. After that, the samples transferred to another furnace to be quenched on molds of stainless steel for annealing process at 220 $^oC$ for 2 hrs., then the furnace was switched off and the samples were allowed to cool.

### 2.2. Characterization and devices

X-ray diffraction (XRD) was performed in this study using X-ray (Shimadzu D6000) diffraction, using $CuK_\alpha$radiation at 40 KV in the 2θ range from $10^o$ to $80^o$ with a step of $0.02^o$ 2θone second for each step, at 1.5418 Å, at ambient temperature, in the air.

The vertical (vv) polarized spontaneous Raman spectra of the prepared glass was acquired by using a thermo scientific DXR Raman Microscope Spectroscopy setup excitation [532 nm Laser Type Diode – Pumped, Solid State (DPSS)] and acquisition time was set to 30 seconds having an output laser power of 10 mW. The incoming signal vertically surfaces of the bulk sample, and V– polarized Raman scattered signal was collected in the backscattering geometry with a 100x microscope objective.

The densities of the prepared glassy samples were determined at room temperature with repeated measurements by the Archimedes method using toluene as the immersion liquid, and a sensitive digital balance $10^{-4}$g. Using the following equation

$$\rho_{glass} = \left(\frac{W}{W-W_L}\right)\rho_L \quad (1)$$

whereW and $W_L$are the weights of the glass sample in air and toluene respectively, $\rho_L$ is the density of toluene (0.865 $g.cm^{-3}$).

The molar volume V could be calculated according to the following relation

$$V = \frac{M_{glass}}{\rho_{glass}} \quad (2)$$

$$M_{glass} = (0.9 - x)M_{(TeO_2)} + xM_{(V_2O_5)} + 0.1M_{(Li_2O)} \quad (3)$$

where$M_{glass}$ and $\rho_{glass}$are the mass and density of the glass sample, respectively.

Oxygen molar volume $V_o$has been calculated following the expression

$$V_o = \left(\sum \frac{x_i M_i}{\rho}\right).\left(\frac{1}{\sum x_i n_i}\right) \quad (3)$$

where$x_i$is the molar fraction of each component i, and $n_i$is the number of oxygen atoms in each oxide.

Oxygen packing density(O.P.D.) was calculated by

$$O.P.D. = \frac{1000.\rho.N_o}{M} \quad (4)$$

where$N_o$is the number of oxygen atoms per formula and $M$ is the molecular weight.

The microhardness measurements were performed using Vickers method.$H_v$was measured via Reichert metallurgical microscope (MeF, Austria) adapted for this purpose. A total of 10 readings distributed over the whole surface of the sample using an indentation time of 10 seconds and an indentation load 0.5 N. the error in $H_v$ arises from the measurements of the diagonal impression not more than ± 3%. The measurements were performed in air at room temperature.

$H_v$was computed using the equation

$$H_V = 1.8544\frac{F}{d^2} \quad (5)$$

whereF is the load, and d is the average of diagonal length.

## 3. Results and discussion

### 3.1. XRD Characterization

The structure of the glass systems was checked by means of x-ray diffraction. The obtained diffraction patterns are shown in Fig (1), it is observed that there is no peak created which confirmed the amorphous nature of the synthesized glasses. The presence of a broad hump over the region $20^o$ – $40^o$ indicates that prepared glass materials have under structure relaxation and phase transformationinside the glass zone [25]. The hump location displays the location of the peak that will be created if the glass starts to crystallize [26].This phenomenon also is shown in other glasses such as $Sb_2O_3$ – $TeO_2$ – $V_2O_5$ [27], and MO – $TeO_2$ – $V_2O_5$ [28].

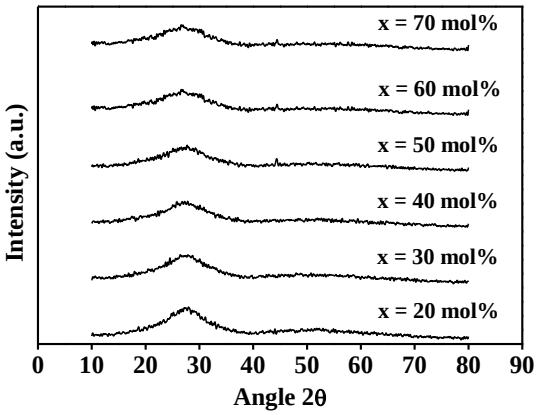


*Fig. 1. XRD patterns for the [(90 – x) $TeO_2$ – (x)$V_2O_5$ – 10$Li_2O$] Glass Materials where (x = 20, 30, 40, 50, 60 and 70 mol%).*

### 3.2. Raman Spectra Analysis

Raman spectral measurements were performed into the synthesized glasses to get more insight about the structural arrangements and identify the presence of various molecular units. Experimental Raman spectra of the [(90 – x) $TeO_2$ – (x)$V_2O_5$ – 10$Li_2O$] glassy system at room temperature in the range (100 $cm^{-1}$ – 1200 $cm^{-1}$) is presented in Fig. (2). The bands in the Raman spectra are broad and shoulders which are attributed to the disorder of the glass structure. Therefore, Raman spectral bandsare deconvoluted for each glass into several symmetrical Gaussian functions to detect the molecular vibrations and structural units. The deconvoluted spectra are divided into three regions 100 $cm^{-1}$ – 560 $cm^{-1}$, 560 $cm^{-1}$ – 890 $cm^{-1}$ and > 890 $cm^{-1}$ and presented on Fig. (3(a-f)).Table 1 Indicates Raman band positions and assignment of the glass systems.

*Table 1. Indicates Raman Band Positions and Assignment for the [(90 – x) $TeO_2$ – (x)$V_2O_5$ – 10$Li_2O$] Glasses.*

| Region | Raman Band | Assignment |
|---|---|---|
| **I** | ~ 205 – 404 $cm^{-1}$ | Assigned to vibrations of trigonal pyramidal (tp) $TeO_3$ groups overlapped with V – O – V and/or V – O – Te vibrations |
| | 471 – 483 $cm^{-1}$ | Assigned to symmetric stretching vibrations of Te – O – Te linkages in the $TeO_4$ (tbp) |
| | 514 $cm^{-1}$ | Associated with the structural changes of the Te – O units or with the increase of O – V – O bonds |
| **II** | 650 – 690 $cm^{-1}$ | Assigned to stretching vibrations of Te - $O_{ax}$ in $TeO_4$ (tbp) units |
| | 801 – 810 $cm^{-1}$ | Assigned stretching vibrations of Te – O in TeO3 (tp) units |
| **III** | 926 – 949 $cm^{-1}$ | Assigned to the O – V – O and V – O – V stretching vibration in $VO_4$ units |
| | 969 – 999 $cm^{-1}$ | Assigned to V = O vibrations in $VO_5$ tetragonal pyramid units |

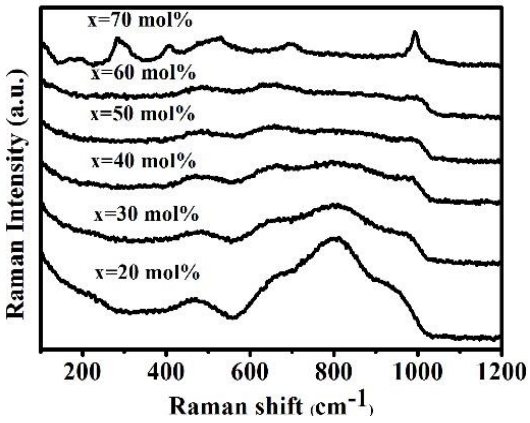


*Fig. 2. The Raman spectra for the [(90 – x) $TeO_2$ – (x)$V_2O_5$ – 10$Li_2O$] Glass Materials where (x = 20, 30, 40, 50, 60 and 70 mol%).*

The Raman spectrum of pure $TeO_2$ glass and for different $TeO_2$ – based glasses in a wide range compositions and systems studied by various authors [29,30] shows a band at 300 $cm^{-1}$ which is attributed to the vibration of $TeO_3$, the band at425 $cm^{-1}$ – 597 $cm^{-1}$assigned to stretching bending vibrations of Te – O – Te or O – Te – O linkages formed by corner-sharing of $TeO_4$ (tbp), $TeO_{3+1}$polyhedra, and $TeO_3$ (tp) structural units, the band 581 $cm^{-1}$ – 623 $cm^{-1}$ attributed to stretching vibrations of Te – O bonds of $TeO_4$ (tbp) units, the band 648 $cm^{-1}$ – 700 $cm^{-1}$referred to stretching vibrations of Te - $O_{ax}$ in $TeO_4$ (tbp) units, the band 716 $cm^{-1}$ – 753 $cm^{-1}$referred to stretching vibrations of Te – O in $TeO_3$ (tp) units, and the band 773 $cm^{-1}$ – 793 $cm^{-1}$assigned to stretching vibrations of non – bridging Te – $O^-$ bonds in $TeO_3$ (tp) units.

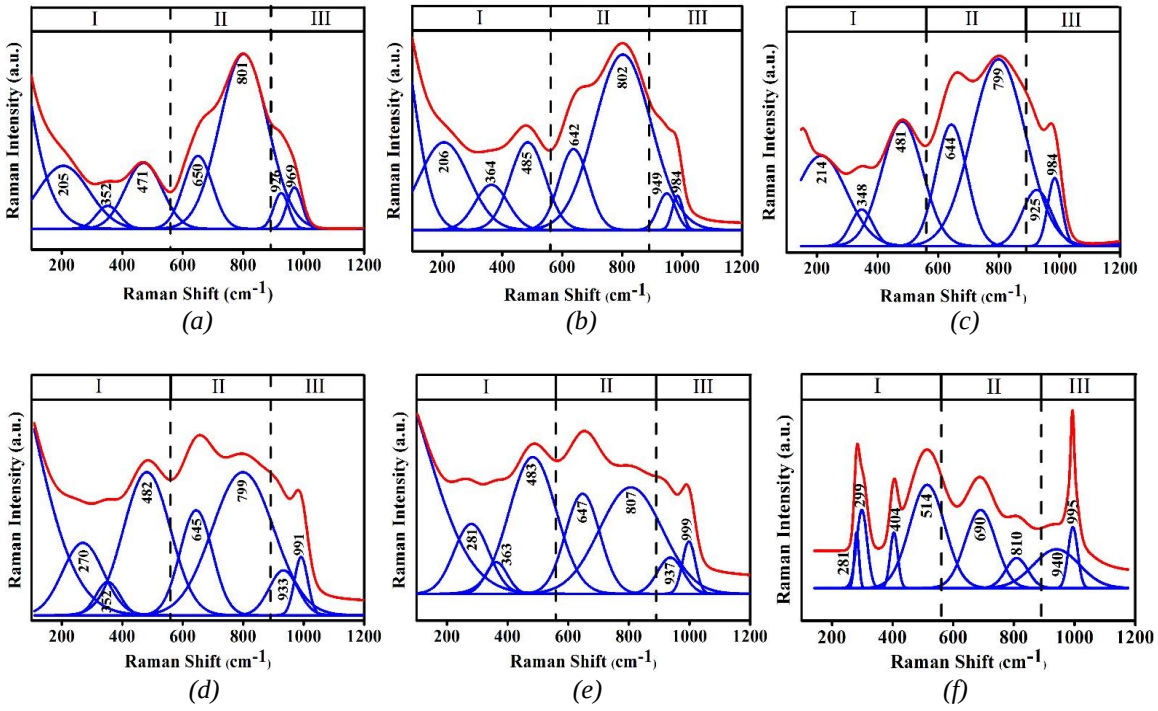


*Fig. 3. The Deconvoluted Raman spectra for (a) 70$TeO_2$ – 20$V_2O_5$ – 10$Li_2O$, (b) 60$TeO_2$ – 30$V_2O_5$ – 10$Li_2O$, (c) 50$TeO_2$ – 40$V_2O_5$ – 10$Li_2O$, (d) 40$TeO_2$ – 50$V_2O_5$ – 10$Li_2O$, (e) 30$TeO_2$ – 60$V_2O_5$ – 10$Li_2O$, (f) 20$TeO_2$ – 70$V_2O_5$ – 10$Li_2O$ Glass Materials.*

In case of pure $V_2O_5$glass it has been reported [31] that $V^{5+}$ ions exhibit both four – and five-fold coordination states, depending on the conditions of sample preparation. The Raman spectrum of amorphous $V_2O_5$ is characterized by the band in the 910 $cm^{-1}$ – 950 $cm^{-1}$ range, related to stretching vibration in $VO_4$ units, while the band in the range 960 $cm^{-1}$ – 1000 $cm^{-1}$ was related to vibration in $VO_5$ trigonal bipyramids [32].

In $TeO_2 – V_2O_5$ binary glasses the basic structural units are $TeO_4$ (tbp), $TeO_{3+1}$ polyhedra, $TeO_3$ (tp), $VO_4$ tetrahedra, and $VO_5$ trigonal bipyramids [15]. L. Baia et al. [33] studied the structure of $xV_2O_5$ $(1 – x)$ $TeO_2$, showed that, by increasing the $V_2O_5$ content, a transformation of some $TeO_4$ units into $TeO_{3+1}$ polyhedra and $TeO_3$ units have been observed. The ratio $V^{4+}/ (V^{4+} + V^{5+})$ decreases with increasing $V_2O_5$ content, and the $V^{5+}$ cations are incorporated in the glass network as $VO_4$ tetrahedra and $VO_5$ trigonal bipyramids.

The physical properties of ternary Telluro – vanadate glasses depending on the third oxide components. Addition of a second transition metal oxide or rare – earth oxide was suggested to increase rigidity of the glasses by the formation bridging oxygens (BO) as reported in studied onthe glassy system $xCuO – 65TeO_2 – (35 – x)$ $V_2O_5 \leq x \leq 10$ mol%by Yahia et al. [34], using infrared (IR) and Raman spectroscopies. Showing that, the presence of four main absorption bands attributed to $TeO_3$, $TeO_4$, $VO_4$, and $VO_5$ structure units. Concluded that, by increasing the content of CuO, it suggestedan increase in the transformation of$TeO_3$ to $TeO_4$, and $VO_5$ to $VO_4$. On the contrary, structural studies on the addition of monovalent oxides was suggested to increase the number of non – bridging oxygens (NBO) in the ternary tellurovanadate glass system, as reported in studies on $(65 – x)$ $V_2O_5 – xBi_2O_3 – 35TeO_2$ system (x = 7.5, 10, 12.5 and 15 mol%) by Rahim [35], using FTIR and Raman spectroscopies. Analysis of the deconvoluted peaks in FTIR and Raman spectra of the glasses found that, the existence of $TeO_4$, $TeO_{3+1}$, $VO_5$, $VO_4$, and $BiO_6$ units. Concluded that, by increasing the amount of $Bi_2O_3$ promotes the conversion of $VO_5$ into $VO_4$, and $TeO_4$ to $TeO_{3+1}$ structure unit having one nonbridging oxygen atom.

In region I (100 $cm^{-1}$ – 560 $cm^{-1}$) Raman peaks of the glasses observed at ~ 205 $cm^{-1}$ – 404 $cm^{-1}$ can be assigned to vibrations of trigonal pyramidal (tp) $TeO_3$ groups overlapped with V – O – V and / or V – O – Te vibrations [21]. As the peaks become less intense with increasing $V_2O_5$ content it is likely that the contribution of $TeO_3$ (tp) structural unit decreases with increasing of $V_2O_5$ content.The presence of the band, which shifts to the higher wavenumbers from 471 $cm^{-1}$ to 483 $cm^{-1}$, can be concluded from the experimental Raman spectra of collected samples with increasing $V_2O_5$ content, in the region between 100 $cm^{-1}$ and 560 $cm^{-1}$ Fig. (2). After applying the deconvolution procedure Fig. (3(a-f)), the band can be assigned to symmetric stretching vibrations of Te – O – Te linkages in the $TeO_4$(tbp) [36]. The shift of this band is due to the distortion of $TeO_4$ units by increasing $V_2O_5$ content. this means that the connectivity of the glass former network Te – O bonds are reduced. The band around 514 $cm^{-1}$, can be associated with the structural changes of the Te – O units or with the increase of O – V – O bonds [21].

Moreover, in the frequency region II between 560 $cm^{-1}$ and 890 $cm^{-1}$ additional bands have been also revealed. The main band, which appeared on the spectrum of $70TeO_2 – 20V_2O_5 – 10Li_2O$ sample, occurs at 801 $cm^{-1}$ and moves slightly to higher wavenumbers with the addition of $V_2O_5$ Fig. (2). It can be noticed on the spectrum of $70TeO_2 – 20V_2O_5 – 10Li_2O$, characterized by the substantial band at 650 $cm^{-1}$ Fig. (2). Deconvoluted spectra of glass samples presented in Fig. (3(a-f)) exposes the presence of two bands in the frequency region 560 $cm^{-1}$ – 890 $cm^{-1}$, located at 650 $cm^{-1}$ and 801 $cm^{-1}$. Comparing deconvoluted spectra substantial change in their assigned positions is being indicated. Thus, the structure of the glass materials varies extensively as $V_2O_5$ increased.The first peak observed at around 650 $cm^{-1}$ – 690 $cm^{-1}$, it can be ascribed to stretching vibrations of Te – $O_{ax}$in $TeO_4$(tbp) units [34]. The second revealed band is located at 801 $cm^{-1}$– 810 $cm^{-1}$ on the deconvoluted spectra of the glass samples Fig. (3(a-f)). Its relative intensity is higher than in comparison to the features of a band at 650 $cm^{-1}$, the assignment of this band attributed to stretching vibrations of Te – O in $TeO_3$(tp) units respectively [34]. As the$V_2O_5$content increases, progressive changes in the structure are observed on deconvoluted spectra. The intensity of the band centered at about 650 $cm^{-1}$ decreased slower than the intensity of the band at 801 $cm^{-1}$. This is described to the Tepolyhedron structure tends to the transformation of nonbridging oxygens $TeO_3$(tbp) into bridging oxygens $TeO_4$ (tp) structural units via $TeO_{3+1}$ polyhedra [34].

On the other hand, at high-frequency region (region III), the bands at 926 $cm^{-1}$ and 969 $cm^{-1}$ have been exposed. Addition of $V_2O_5$ content increasing in intensity and shifting to higher wavenumbers from 926 $cm^{-1}$ Fig.(3a) to 940 $cm^{-1}$ Fig. (3f) is observed for the first one. This band is not present in the spectra of tellurite glasses containing network modifier and can be clearly assigned to the V – O structural units. Then, it is particularly assigned to V = O vibration in the tetragonal pyramid of $V_2O_5$ [33], indicates that the glass network consists of both $VO_4$ tetrahedra and $VO_5$ tetragonal pyramids. Furthermore, the increasing intensity of the band at ~ 926 $cm^{-1}$ assigned to the O–V–O and V–O–V groups in $VO_4$ lead to the breaking of the tellurite chains and $V_2O_5$ tend to act as a network former [36].The location of the second band also shifts towards higher wavenumbers, starting with ~ 969 $cm^{-1}$ in a $70TeO_2 – 20V_2O_5 – 10Li_2O$ spectrum Fig. (3a), reaching the value ~ 995 in a $20TeO_2 – 70V_2O_5 – 10Li_2O$ spectrum Fig. (3f), indicates the presence of $VO_5$ tetragonal pyramids [35]. The deconvoluted Raman spectra show that, the area of the $VO_4$ band increases greater than that for $VO_5$ band, which shows that some $VO_5$ units transformed in the structural unit of $VO_4$ units.

Insertion of $Li_2O$ on the expense of $TeO_2$ leads to a shift of the Raman bands of the base glass (telluro vanadate glass) to higher wavenumber and lower relative area. This could be attributed to the higher band strength and lower ionic radii of $Li_2O$ than that of $TeO_2$ [37]. Increasing the vanadate content at constant $Li_2O$ content, on the expense of $TeO_2$ content causes the principal bands of vanadate to shift to higher wavenumber and to the higher relative area [37].

### 3.3.Density Measurements and Molar Volume

Density is an additive property; the substitutes alter the places without interaction with the neighboring environments. In other words, the density is related to the packing of ions and atoms in the structure. In tellurovanadate glasses, as vanadium put into the glass, it surrounded by tellurium bipyramids. With increasing the concentration of vanadium, the possibility of detecting another vanadium bipyramid increases.

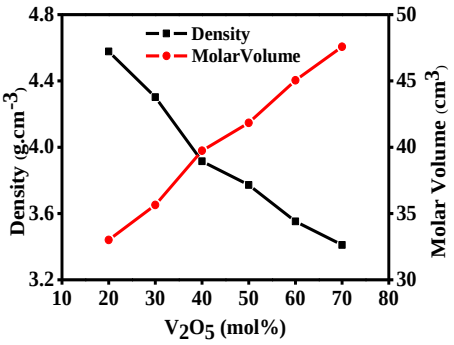


*Fig. 4. Density (ρ) and Molar Volume for the [(90 – x) $TeO_2$ – (x)$V_2O_5$ – 10$Li_2O$] Glass Materials where (x = 20, 30, 40, 50, 60 and 70 mol%).*

The physical properties of the glasses system [(90 – x) $TeO_2$ – (x)$V_2O_5$ – 10$Li_2O$] with different concentration of $V_2O_5$ from 20 up to 70 mol%, were investigated by measuring the densities of the glass samples. Fig (4) shows the variation of the density of the ternary glass system and $V_2O_5$ mol% concentration and the exact values were collected in the table (2). It can be seen from the figure that the density decreases from 4.58 to 3.41 $g.cm^{-3}$ with an increase in $V_2O_5$ content range from 20 to 70 mol%. The density of the present tellurite glasses is slightly greater than that reported of ternary $TeO_2 – V_2O_5 – K_2O$[21], and close to $Gd_2O_3 – TeO_2 – V_2O_5$ [36]. The decrease in the density is related to the replacement of high dense $TeO_2$ (5.67 $g.cm^{-3}$) with low dense on $V_2O_5$ (3.3 $g.cm^{-3}$), i.e. the decrease of the glass density as a function of composition is attributed to the structural rearrangement of atoms inside the glass by increasing the $V_2O_5$ content.

*Table 2. Values of density ρ, molar volume V, oxygen molar volume $V_o$, oxygen packing density (O.P.D.) and microhardness (H.V.) for [(90 – x) $TeO_2$ – (x)$V_2O_5$ – 10$Li_2O$] glass materials where (x = 20, 30, 40, 50, 60 and 70 mol%).*

| $V_2O_5$ (mol%) | $\rho_{exp.}$ ($g.cm^{-3}$) | $\rho_{calc.}$ ($g.cm^{-3}$) | V ($cm^3$) | $V_o$ ($cm^3.mol^{-1}$) | O.P.D. ($g.atm.L^{-1}$) | $d_{v-v}$ (nm) | H.V. (MPa) |
|---|---|---|---|---|---|---|---|
| 20 | 4.578 | 4.840 | 33.001 | 12.807 | 75.755 | 32.47 | 3189 |
| 30 | 4.302 | 4.608 | 35.641 | 12.362 | 78.561 | 34.83 | 3056 |
| 40 | 3.915 | 4.376 | 39.734 | 12.004 | 78.019 | 38.02 | 2639 |
| 50 | 3.772 | 4.144 | 41.832 | 11.709 | 81.279 | 41.11 | 2505 |
| 60 | 3.552 | 3.912 | 45.041 | 11.462 | 82.147 | 45.38 | 2393 |
| 70 | 3.410 | 3.680 | 47.572 | 11.252 | 84.084 | 50.87 | 2253 |

The density was calculated theoretically using the relation [38]

$$\rho_{calc.} = \sum_i x_i \rho_i \qquad (6)$$

where $x_i$ and $\rho_i$ are the molar fraction and density for each component, respectively. From table (2), the measured densities experimentally and theoretically have the same behavior, which decreased by increasing $V_2O_5$ content. The difference between the experimental andtheoretical densities values, may be due to the change in the glass chemical composition through the melting process [38].

The molar volume V is a measure of the network compactness. Fig (4) shows that, the variation of the molar volume V of the present ternary glass with $V_2O_5$ mol% concentration. The molar volume of these systems increases from 33.0 to 47.57 $cm^3$ with increasing $V_2O_5$ as shown in the table (2). The molecular weight of $TeO_2$ (159.6 g/mol) is lower than that of $V_2O_5$ (181.88 g/mol), thus the molar volume of the glasses increases as $V_2O_5$ replaces $TeO_2$ inside the glass matrix. Swapna et al. [39] reported that, the increase in molar volume indicates that these glasses have a more disordered structure due to the increase in the free volume. Changes in molar volume are attributed to changes in structure caused by an increase in interatomic spacing, which in turn decreases the stretching force constant of the bonds inside the glassy network, resulting in less compact glass[39].

On the other hand, the trend of density and molar volume can be explained due to the replacement of heavier cation (V) by a lighter cation (Te). As observed in Raman spectra, the addition of $V_2O_5$ causes an increase in NBOs, that randomizes the structure and, therefore, the glass network becomes more open. Then, non – bridging oxygens (NBOs) created in the glass due to the increase of $V_2O_5$ content, which shows that $VO_4$(NBOs) grow faster than $V_2O_5$(BOs) by increasing $V_2O_5$ content. These results are consistent with early reported results [26].

Fig (5) shows the variation of oxygen molar volume $V_o$ with $V_2O_5$ mol% content. The oxygen molar volume decreases from 12.81 to 11.25 $cm^3$ with increasing $V_2O_5$ as shown in the table (2). The change in both V and $V_o$ are contributed to the molecular weight of constituents in the glass composition, the number of an oxygen atom, the cation radius and the coordination number. The decrease of oxygen molar volume indicates structural packing in the glass network, oxygen packing density which is a measure of the tightness of packing of oxide network. It can be seen from Fig(5) and table (2) that, oxygen packing density increases as the concentration of $V_2O_5$ increases. This indicates that the structure becomes more tightly packed when more $V_2O_5$ is incorporated into the vitreous matrix.

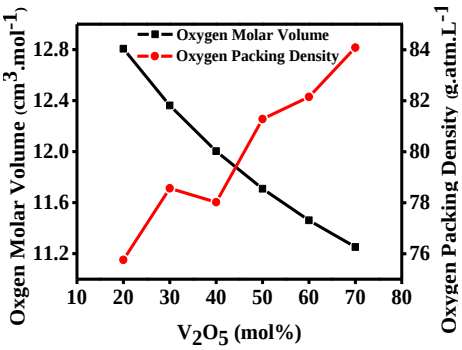


*Fig. 5. Oxygen molar volume ($V_o$) and the Oxygen Packing Density for the [(90 – x) $TeO_2$ – (x)$V_2O_5$ – 10$Li_2O$] Glass Materials where (x = 20, 30, 40, 50, 60 and 70 mol%).*

The obtained decrease in oxygen molar volume is associated with an increase in oxygen packing density. It confirms the formation of non – bridging oxygen bonds by replacement of $TeO_2$ with $V_2O_5$ content up to 70 mol%. This is may be related to the formation of $VO_4$ tetrahedral units, by conversion of $VO_5$ structural units to $VO_4$ units. This state is responsible for increasing the non – bridging oxygen bonds. The gradual conversion of $VO_5$ to $VO_4$, acts $VO_4$ as a modifier, which breaks up the local symmetry and introduces coordinated defects into the synthesized glass.

To get more appreciation on the glass network modification due to the increase in the concentration in $V_2O_5$, the average vanadium interatomic spacing $d_{v\text{-}v}$ was calculated, by the relation [40]

$$d_{v-v} = \left(\frac{V_v}{N_A}\right)^{1/3} \tag{7}$$

where$V_v$ is the vanadium molar volume, and $N_A$ is the Avogadro's number (6.023 x $10^{23}$ g/mol). The vanadium molar volume, is the volume that contains one mole of vanadium atoms within the glass structure, is found using the relation

$$V_v = \frac{V}{2(1-x_v)} \tag{8}$$

where $x_v$ is $V_2O_5$ molar fraction. Therefore, the calculated values of vanadium – vanadium separation $d_{v\text{-}v}$are increased by increasing $V_2O_5$ content from 32.47 nm to 50.87 nm. Then, the increase in the concentration of $V_2O_5$ leads to expansion of the glass structure which emphasis the results of density and molar volume.

### 3.4. Microhardness Measurements

Microhardness indicate the stress required to remove the free volume (the network deformation) of the glass. Vicker's hardness measurements were accomplished for the prepared glasses and the values lie between 3189 to 2253 MPa, as tabulated in the table (2). The variation of microhardness of [(90 – x) $TeO_2$ – (x)$V_2O_5$ – 10$Li_2O$] glasses as a function of $V_2O_5$mol% shown in Fig. (6). The microhardness decreases with increasing $V_2O_5$ content in the glass network and could be attributed to the creation of non – bridging oxygens in the glass, which needs less energy for breaking the bond in the network. The decrease in the microhardness indicates the decreasein the rigidity of the glass [41]. Shelby [42] showed that, in x$V_2O_5$ – 20SnO – (80 – x) $TeO_2$ series of glasses. The covalency of the V – O bond in x$V_2O_5$ – 20SnO – (80 – x) $TeO_2$ glasses should decrease with an increase in $V_2O_5$ mol%. The decrease in covalency increases the number of non – bridging oxygens in the glass. The increase in the concentration of non – bridging oxygens reduces the connectivity of the glassy network which decreases the microhardness of the glass system.

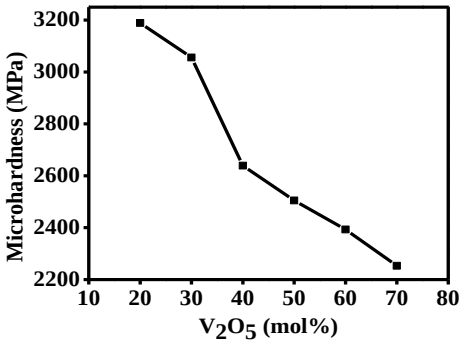


*Fig. 6.Microhardness (H.V.) for the [(90 – x) $TeO_2$ – (x)$V_2O_5$ – 10$Li_2O$] Glass Materials where (x = 20, 30, 40, 50, 60 and 70 mol%).*

## 4. Conclusion

The XRD of the samples under investigation, that was prepared via melt-quenching technique, shows the amorphous nature and this is confirmed by Raman spectroscopy. The density of the samples decreases from 4.58 to 3.41 $g.cm^{-3}$ with rising of $V_2O_5$ content range from 20 to 70 mol%, respectively. Moreover, the oxygen molar volume, also, decreased from 12.81 to 11.25 $cm^3$. Due to the microhardness results of the glass system, the rigidity decreased.

**Acknowledgement**

This research was supported by the Deanship of Scientific Research, King Khalid University, Abha, Saudi Arabia (award number R.G.P.1/130/40).

## References

[1] E.S. Yousef, Journal of Alloys Compounds **561**,234 (2013).
[2] M.M. Umair, A.K. Yahya, M.K. Halimah, H.A.A. Sidek, Journal of Materials Science & Technology **31**,83 (2015).
[3] M.S. Gaafar, S. Y. Marzouk, Journal of Alloys and Compounds **723**,1070 (2017).
[4] S.K. Ahmad, M.A. Samee, A.Edukondalu, S. Rahman, Results in Physics **2**,175 (2012).
[5] N. Ghribi, M.D. Coles, J.R. Duclère, T. Hayakawa, J. Carreaud, R. Karray, A. Kabadou, P. Thomas, Journal of Alloys and Compounds **622**,333 (2015).
[6] A.B. Nedeleheva, R. Iordanova, K.L. Kostov, St. Yordanov, V. Ganev, Optical Materials **34**, 1781 (2012).
[7] V. Rodriguez, G. Guery, M. Dussauze, F. Adanietz, T. Cardinal, K. Richardson, The Journal of Physical Chemistry C **120**,23144 (2016).
[8] A. Kaur, A. Khanna, C. Pesquera, F. Gonzalez, V. Sathe, Journal of Non-Crystalline Solids **356**,864 (2010).
[9] E. Culea, I.V. Simiti, G. Borodi, E.N. Culea, R. Stefan, P. Pascuta, Journal of Materials Science **49**,4620 (2014).
[10] G.P. Singh, P. Kaur, S. Kaur, D.P. Singh, Materials Physics and Mechanics **12**,58 (2011).
[11] A. Wagh, Y. Raviprakash, V. Upadhyaya, S.D. Kamath, SpectrochimicaActa Part A: Molecular and Biomolecular Spectroscopy **151**,696 (2015).
[12] N. Gedikoğlu, M.Ç. Ersundu, P. Koska, N. Bašinová, A.E. Ersundu, Journal of Alloys and Compounds 748,687 (2018).
[13] S. Laila, A.K. Suraya, A.K. Yahia, Chalcogenide Letters **11**,91 (2014).

[14] S. Chakraborty, P. Boolchand, M. Malki, M. Micoulaut, The Journal of Chemical Physics **140**,1 (2014).
[15] D. Souri, Y. Shahmoradi, Journal of Thermal Analysis and Calorimetry **129**,601 (2017).
[16] J. Kjeldsen, A.C.M. Rodrigues, S. Mossin, Y. Yue, The Journal of Physical Chemistry B **118**,14942 (2014).
[17] R. Kaur, R. Kaur, A. Khanna, F. González, AIP Conference Proceedings **1942**, 070028 (2018).
[18] D. Souri, S. A. Salehizadeh, Journal of Material Science **44**,5800 (2009).
[19] H.M.M. Moawad, H. Jain, R. El-Mallawany, Journal of Physics and Chemistry of Solids **70**, 224 (2009).
[20] I.S. Yahia, Y.B. Saddeek, G.B. Sakr, W. Knoff, T. Story, N. Romčvić, W. Dobrowlski, Journal of Magnetism and Magnetic Materials **321**,4039 (2009).
[21] S.A. Salehizadeh, B.M.G. Melo, F.N.A. Freire, M.A. Valente, M.P.F. Graça, Journal of Non-Crystalline Solids **443**,65 (2016).
[22] R. Hisam, A.K. Yahya, H.M. Kamari, Z.A. Talib, Ionics **23**,1423 (2017).
[23] N. Krins, A. Rulmont, J. Grandjean, B. Gilbert, L. Lepot, R. Cloots, B. Vertruyen, Solid State Ionics **177**,3147 (2006).
[24] M.A. Frechero, O.V. Quinzani, R.S. Pettigrosso, M. Villar, R.A. Montani, Journal of Non-Crystalline Solids **353**,2919 (2007).
[25] V. Rao, N. Chandel, N. Mehta, D.K. Dwivedi, Journal of Thermal Analysis and Calorimetry **134**,915 (2018).
[26] L. Hasnimulyati, M.K. Halimah, A. Zakatia, S.A. Halim, M. Ishak, C. Eevon, Journal of Ovonic Research **12**,291 (2016).
[27] D. Souri, Z. Torkashvand, Journal of Electronics Materials **46**,2158 (2017).
[28] S. Chen, W. Li, D.G. Zhu, Materials Research Bullletin**101**,29 (2018).
[29] N. Berwal, S. Dhankhar, P. Sharma, R.S. Kundu, R. Punia, N. Kishore, Journal of Molecular Structure **1127**,636 (2017).
[30] N.S. Tagiara, D. Palles, E.D. Simandiras, V. Psycharis, A. Kyritsis, E.I. Kamitsos, Journal of Non – Crystalline Solids **457**,116 (2017).
[31] S. Rada, M. Neumann, E. Culea, Solid State Ionics **181**,1164 (2010).
[32] N. Kerkouri, M. Ettabirou, A. Chahine, A. Mazzah, M.C. Dhamelincouri, M. Taibi, J. Optoelectron.Adv. M.**12**,1030 (2010).
[33] L. Baia, M. Bolboaca, W. Kiefer, E.S. Yousef, C. Rüssel, F.W. Breitbarth, T.G. Mayerhöfer, J. Popp, Physical Chemistry Glasses **45**(3),178 (2004).
[34] I.S. Yahia, Y. B. Saddeek, G.B. Sakr, W. Knoff, T. Story, N. Romčvić, W. Dobrowlski, Journal of Magnetism and Magnetic Materials **321**,4039 (2009).
[35] A.S. Rahim, A.K. Arof, Optical and Quantum Electronics **48**, 238 (2016).
[36] Y.B. Saddeek, I.S. Syahia, W. Dobrowolski, L. Kilanski, N. Romcevic, M. Arciszewska, Optoelectron. Adv. Mat.**3**,559 (2009).
[37] Y.B. Saddeek, E.R. Shaaban, K.A. Aly, I.M. Sayed, Journal of Alloys and Compounds **478**,447 (2009).
[38] H.A. Othman, H.S. Elkholy, I. Z. Hager, Journal of Molecular Structure **1106**,286 (2016).
[39] Swapna, G. Upender, M. Prasad, Journal of Taibah University for Science **11**,583 (2017).
[40] F.A. Moustafa, M. Abdel – Baki, A. M. Fouad, F. El – Diasty, American Journal of American Science **4**,119 (2014).
[41] M.K. Halimah, W.M. Daud, H.A. A. Sidek, Ionics **16**,807 (2010).
[42] J.E. Shelby, "Introduction to Glass Science and Technology", RSC, UK, 1997.